

## Research Article

# Nafion®-Containing Solid Lipid Nanoparticles as a Tool for Anticancer Pt Delivery: Preliminary Studies

Maddalena Sguizzato,<sup>1</sup> Elisabetta Esposito,<sup>1</sup> Marcus Drechsler,<sup>2</sup> Eleonora Gallerani,<sup>1</sup> Riccardo Gavioli,<sup>1</sup> Paolo Mariani,<sup>3</sup> Federica Carducci,<sup>3</sup> Rita Cortesi,<sup>1</sup> and Paola Bergamini<sup>4</sup>

<sup>1</sup>Department of Life Sciences and Biotechnology, University of Ferrara, Ferrara, Italy

<sup>2</sup>BIMF/Soft Matter Electronmicroscopy, University of Bayreuth, Bayreuth, Germany

<sup>3</sup>Department of Life and Environmental Sciences, Università Politecnica delle Marche, Ancona, Italy

<sup>4</sup>Department of Chemical and Pharmaceutical Sciences, University of Ferrara, Ferrara, Italy

Correspondence should be addressed to Rita Cortesi; [crt@unife.it](mailto:crt@unife.it)

Received 10 January 2017; Accepted 1 March 2017; Published 23 March 2017

Academic Editor: Antonio M. Romerosa-Nievas

Copyright © 2017 Maddalena Sguizzato et al. This is an open access article distributed under the Creative Commons Attribution License, which permits unrestricted use, distribution, and reproduction in any medium, provided the original work is properly cited.

Preliminary studies of nanoparticles based on the perfluorosulfonic acid resin Nafion have been carried out with the aim of establishing an ionic connection with the protonable phosphine 1,3,5-triaza-7-phosphaadamantane (PTA), suitable for the coordination of platinum. Nafion-containing nanoparticles (NAF) were produced by homogenization followed by ultrasonication method. After production, NAF were characterized in terms of size, morphology, and *in vitro* cytotoxicity. The PCS studies showed that the Z-average mean diameter was around 250 nm. Moreover, the polydispersity index showed a monodimensional distribution of nanoparticles. Cryo-TEM analysis showed a uniform and homogenous population of particles, characterized by the presence of both ovoidal and needle-like structures. To evaluate the *in vitro* cytotoxicity, NAF were tested on human cancer cell lines K562 and A2780. No cytotoxic effect was found on both cell lines. By <sup>13</sup>P-NMR measures, it is here proved that the strongly acidic sulfonic groups of Nafion-containing nanoparticles (NAF) can act as protonating agents for PTA. The protonation occurs selectively at nitrogen; hence protonated PTA maintains its ability to coordinate platinum via its phosphorus atom.

## 1. Introduction

The amino Pt complexes like cisplatin and analogues are widely used in medical oncology for management of tumors of the ovary, testes, head, and neck and other cancers [1, 2]. An extensive search for platinum-based drugs with improved pharmacological properties and a wider spectrum of action as compared to cisplatin has been developed. It has been supposed that the distribution and the concentration of platinum-based drugs in different body districts are influenced by physicochemical properties of the ligands such as polarity, hydrophilicity, and steric requirements [3]. Among several other modifications, the possibility of structurally modifying cisplatin by introducing phosphines as neutral ligands has been considered [4, 5].

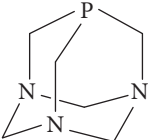
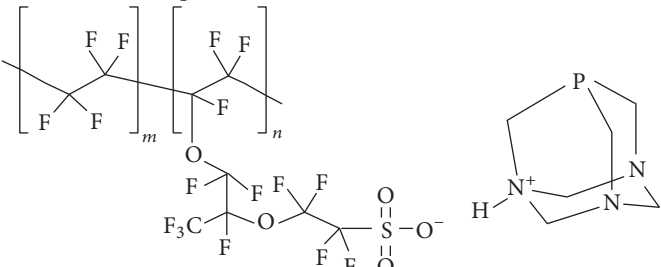
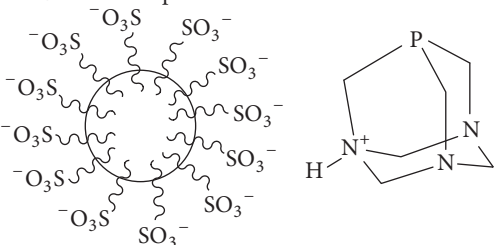
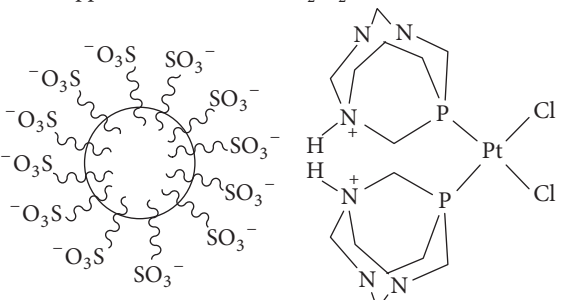
The search of a strategy aimed to the extension of Pt pharmaceutical application to phosphinic complexes has

attracted great interest since many years. To this purpose nanoparticulate drug delivery systems have been considered since they can improve the permeability, safety, pharmacokinetics properties, and bioavailability of the therapeutic substances in the treatment of tumor cells [6].

The phosphine 1,3,5-triaza-7-phosphaadamantane (PTA) (see Table 1) [7] looks particularly suitable for pharmaceutical application because it possesses reactivity and size comparable to that of alkylphosphines [8] with the addition of valuable properties like hydrosolubility, stability to oxidation, and lack of toxicity.

PTA can be selectively alkylated or protonated on nitrogen, thus maintaining its coordinative ability, which is achieved by phosphorus. N-alkylated PTA derivatives can also be introduced as ligands in platinum or ruthenium complexes designed for anticancer activity [9, 10].

TABLE I:  $^{31}\text{P}$  NMR data in  $\text{D}_2\text{O}$ .

	Chemical shift (ppm)
PTA in water 	-100
Nafion + PTA in aqueous solution 	-90.7
NAF/PTAH <sup>+</sup> suspension 	-90.6
NAF-supported <i>cis</i> -[Pt(PTAH <sup>+</sup> ) <sub>2</sub> Cl <sub>2</sub> ] 	-49.5

We recently proposed a delivery system for Pt-PTA complexes based on the use of solid lipid nanoparticles (SLN) of stearic acid that should favour both the delivery and the activity of the Pt-PTA moiety [11].

As an alternative route for including Pt-PTA complexes in solid lipid nanoparticles, in this paper we considered the formation of an electrostatic interaction between appropriate proton donating functionalities and the proton acceptor nitrogen of PTA. To this purpose the fluoropolymer-copolymer Nafion (Table 1) was evaluated.

Nafion is a perfluorinated polymer that contains small proportions of sulfonic functional groups. Although the exact structure of Nafion is not known, its structure can be resembled to that of an ionic surfactant in which the hydrophilic head is typified by the sulfonic functional groups and the hydrophobic portion by the tetrafluoroethylene structure. In

this view, the use of Nafion in the composition of a lipid based nanoparticles could give rise to the formation of a structure in which the lipophilic portion of Nafion lies inside the lipid core of the particles, while its polar moiety is present on particle's surface. The presence of the sulfonic groups on the surface could thus be used to interact with Pt-coordinated PTA.

Particularly, the present study reports (i) the preparation of Nafion-containing nanoparticles (NAF), (ii) their characterization in terms of size, morphology, and X-ray diffraction, (iii) the test of their cytotoxic activity *in vitro* on two different human cancer cell lines, namely, erythroleukemic K562 and ovarian cancer A2780 cells, and (iv) the  $^{31}\text{P}$  NMR investigation of the ability of NAF to selectively protonate PTA on nitrogen and of the coordination ability of the NAF/PTAH<sup>+</sup> system to Pt.

## 2. Materials and Methods

**2.1. Materials.** Tristearin, stearic triglyceride (tristearin), was provided by Fluka (Buchs, Switzerland). Lutrol F 68, methyl-oxirane polymer (75:30) (poloxamer 188) was a gift of BASF ChemTrade GmbH (Burgbernheim, Germany). Nafion was purchased from Sigma-Aldrich (Saint Louis, Missouri, USA).

**2.2.  $^{31}\text{P}$  NMR Analyses.** NMR spectra were recorded using a Varian Gemini 300 MHz spectrometer ( $^{31}\text{P}$  at 121.50 MHz). The  $^{31}\text{P}$  spectra were run with proton decoupling and  $^{31}\text{P}$  signals are reported in ppm relative to an external 85%  $\text{H}_3\text{PO}_4$  standard. No deuterated solvent is required. An internal capillary containing  $\text{C}_6\text{D}_6$  placed inside the tube provides the deuterium necessary for the instrument locking.  $^{31}\text{P}$  NMR data are reported in Table 1.

The concentration of  $-\text{SO}_3\text{H}$  groups in NAF was estimated  $9.0 \cdot 10^{-4}$  mol/L. An equimolar amount of PTA was added and the  $^{31}\text{P}$  NMR spectrum was acquired (18 h acquiring time).

Half equivalent of platinum was then added ( $4.5 \cdot 10^{-4}$  mol/L as  $\text{K}_2\text{PtCl}_4$ ) and the  $^{31}\text{P}$  NMR spectrum was acquired (60 h acquiring time).

**2.3. NAF Preparation.** NAF were prepared by homogenization stirring followed by ultrasonication. Briefly a mixture composed of 3.35% w/w of tristearin and 1.65% w/w of Nafion was melted at  $80^\circ\text{C}$ . The mixture concentration was 5% w/w with respect to the total weight of dispersions. To the fused lipid phase 4.75 ml of an aqueous poloxamer 188 solution (2.5% w/w) was added at  $80^\circ\text{C}$  under 15,000 rpm high-speed stirrer for 1 min, using a Ultra Turrax T25 (IKA-Werke GmbH & Co. KG, Staufen, Germany). The emulsion was then subjected to ultrasonication (Microson<sup>TM</sup>, Ultrasonic cell Disruptor) at 7 kHz for 15 min and cooled down to room temperature by placing it in a water bath at  $22^\circ\text{C}$ . NAF dispersions were stored at room temperature.

**2.4. Photon Correlation Spectroscopy (PCS).** Submicron particle size of different batches of nanoparticles was determined using a Zetasizer Nano S90 equipped with a 4 mW helium neon laser with a wavelength output of 633 nm. Glassware was cleaned of dust by washing with detergent and rinsing twice with water for injections. Measurements were made at  $25^\circ\text{C}$  at an angle of  $90^\circ$ . Samples were diluted 1:10 (v/v) with the aqueous phase of each formulation. Each experimental value results from three independent experiments performed in triplicate. Data were interpreted using the "method of cumulants" [12].

**2.5. Cryotransmission Electron Microscopy (Cryo-TEM).** For cryo-TEM studies, a sample droplet of  $2 \mu\text{l}$  was put on a lacey carbon film copper grid (Science Services, Munich), which was hydrophilized by air plasma glow discharge (Solarus 950, Gatan, Munich, Germany) for 30 s. Subsequently, most of the liquid was removed with blotting paper leaving a thin film stretched over the lace holes. The specimens were instantly shock frozen by rapid immersion into liquid ethane cooled to approximately 90 K by liquid nitrogen in a temperature-controlled freezing unit (LEICA EM GP, Germany). The

temperature was monitored and kept constant in the chamber during all the sample preparation steps. The specimen was inserted into a cryotransfer holder (CT3500, Gatan, Munich, Germany) and transferred to a Zeiss/LEO EM922Omega EFTEM (Zeiss Microscopy GmbH, Jena, Germany). Examinations were carried out at temperatures around 90 K. The TEM was operated at an acceleration voltage of 200 kV. Zero-loss filtered images ( $\text{DE} = 0 \text{ eV}$ ) were taken under reduced dose conditions ( $100\text{--}1000 \text{ e/nm}^2$ ). All images were registered digitally by a bottom mounted CCD camera system (Ultrascan 1000, Gatan, Munich, Germany) combined and processed with a digital imaging processing system (Digital Micrograph GMS 1.9, Gatan, Munich, Germany).

**2.6. X-Ray Diffraction.** X-ray diffraction experiments were performed to characterize the inner structure of nanoparticles containing Nafion. A 3.5 kW Philips PW 1830 X-ray generator (Philips, Eindhoven, Netherlands) equipped with a homemade Guinier-type focusing camera operating in vacuum with a bent quartz crystal monochromator ( $\lambda = 1.54 \text{ \AA}$ ) was used. Diffraction patterns were recorded on a GNR Analytical Instruments imaging plate system (GNR Analytical Instruments Group, Novara, Italy). Samples were held in a tight vacuum cylindrical cell provided with thin Mylar windows. Diffraction data were collected at ambient temperature ( $37^\circ\text{C}$ ), using a Haake F3 thermostat (Thermo-Haake, Karlsruhe, Germany) with an accuracy of  $0.1^\circ\text{C}$ .

The position of Bragg peaks detected in the low-angle X-ray diffraction region ( $Q < 0.6 \text{ \AA}^{-1}$ , being  $Q$  the modulus of the scattering vector defined by  $Q = 4\pi \sin \theta / \lambda$ , where  $2\theta$  is the scattering angle) was measured and peak indexing was performed considering the different symmetries commonly observed in lipid phases [13].

**2.7. Growth Inhibition and Antiproliferative Activity Assays.** Cell growth inhibition assays were carried out using human cells, namely, erythroleukemic K562 and ovarian cancer A2780 cell lines. Cells were maintained in RPMI 1640, supplemented with 10% calf serum, penicillin (100 U/mL), streptomycin (100  $\mu\text{g/mL}$ ), and glutamine (2 mM); the pH of the medium was 7.2 and the incubation was at  $37^\circ\text{C}$  in a 5%  $\text{CO}_2$  atmosphere. Cells were routinely passed every three days at 70% of confluence; for the adherent cell lines, 0.05% trypsin-EDTA was used.

The antiproliferative activity of compounds was tested with the MTT assay K562 or A2780 cells were seeded in triplicate in 96-well trays and NAF dispersions were diluted in culture medium to final concentrations ranging from 5 to  $50 \mu\text{M}$ .

Cells were exposed to the formulations for 72 h; then  $25 \mu\text{l}$  of a 3-(4,5-dimethylthiazol-2-yl)2,5-diphenyltetrazolium bromide solution (MTT) (12 mM) was added and incubated for 2 h. Afterwards  $100 \mu\text{l}$  of lysing buffer (50% DMF + 20% SDS, pH 4.7) was added to convert the MTT solution into a violet coloured formazan. After additional 24 h the solution absorbance, proportional to the number of live cells, was measured by spectrophotometer at 570 nm and converted into percentage of growth inhibition [9].

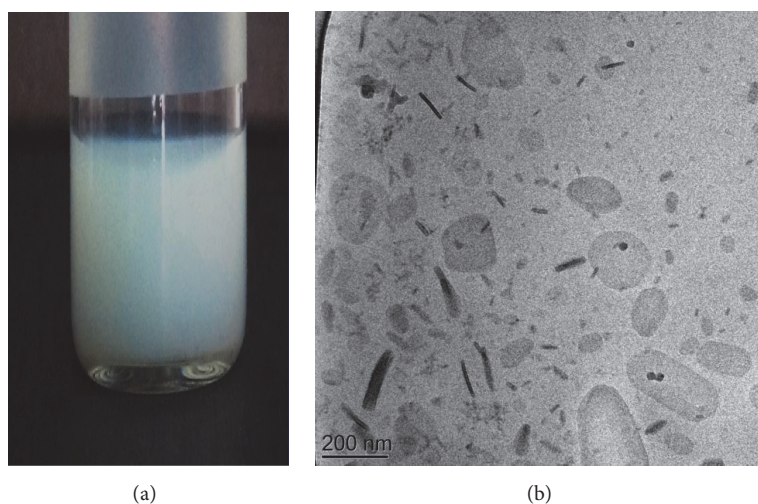


FIGURE 1: Macroscopic aspect (a) and cryotransmission electron microscopy (cryo-TEM) image (b) of the produced NAF.

### 3. Results and Discussion

The formulation of Nafion-containing nanoparticles (NAF) was designed as a tool for loading PTA through the electrostatic interaction between Nafion sulfonic groups (strong proton donors) and the proton acceptor nitrogen atoms of PTA.

The obtained NAF/PTAH<sup>+</sup> system should maintain its ability to coordinate Pt via its P donor atom [14].

As a first point, the ability of Nafion to protonate PTA was checked in water solution by <sup>31</sup>P NMR. It was found that the signal of PTA in water (−100 ppm) is shifted at −90.7 ppm in the presence of Nafion, indicating the complete N-protonation of the phosphine (Table 1).

As a second step it was then necessary to prove that the protonating ability of Nafion is maintained in the NAF formulation.

NAF were produced by homogenization followed by ultrasonication method as described in Materials and Methods. The formulation appeared as a milky white emulsion (see Figure 1), characterized by a uniform appearance with no aggregates and no adherence to the vial's walls. After production, NAF were characterized in terms of morphology and size by cryo-TEM, X-ray diffraction, and PCS analyses.

Cryo-TEM analysis was effectuated to shed light on the internal structures of particles dispersed in plain NAF and Figure 1 shows the resultant image. In general, NAF dispersions are mainly constituted of discoid-shaped structures. Particularly, when viewed from the top, the particles appear as circular or ellipsoidal, or as dark rods or “needles,” depending on particle position and on their thickness. Moreover, some structures evidence the inner lamellar morphology of nanoparticles, probably due to the presence of tristearin mixed with Nafion (liquid at room temperature) resulting in the typical “sandwich-like” appearance.

Figure 2 shows the X-ray diffraction results for nanoparticles without and with NAF. Particularly, nanoparticles without NAF were used for comparison. It was found that X-ray

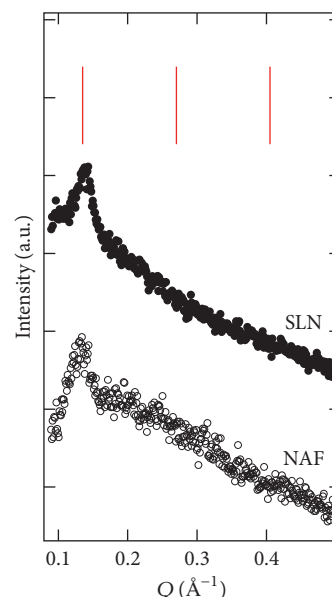


FIGURE 2: X-ray diffraction profiles observed for nanoparticle dispersions without (black dots) and with NAF (white dots) at 37°C. The SLN profile has been shifted for clarity. Vertical lines indicate the position of the first 3 peaks expected in the case of a 1D lamellar symmetry: note that, in the NAF profile, the second order of diffraction is almost appreciable, confirming the lamellar symmetry.

profiles are very similar, with only one peak clearly resolved in the low-angle region. The corresponding unit cell, assuming a lamellar structure, is 49 and 46 Å for nanoparticles with and without NAF. Thus the presence of Nafion does not induce structural modifications in the internal structure of nanoparticles.

Size, polydispersity, and stability of NAF during time were evaluated by PCS analysis. The obtained results are showed in Table 2. The analysis was repeated over a period



TABLE 2: Z-average diameter and polydispersity of NAF during time.

Time (days)	Z-average (nm)	PdI
0	235.8 ± 6.70	0.209 ± 0.04
3	249.0 ± 9.91	0.223 ± 0.02
7	259.8 ± 3.06	0.235 ± 0.03
15	249.3 ± 5.02	0.232 ± 0.03
20	246.8 ± 9.42	0.220 ± 0.03
30	253.3 ± 6.37	0.207 ± 0.02
60	256.7 ± 11.26	0.225 ± 0.04
90	245.7 ± 7.62	0.202 ± 0.03

of three months and during this time the mean diameter was maintained between 230 and 260 nm indicating a dimension of particles according to pharmaceutical literature [15]. Regarding the polydispersity, the indices were stable during time approximately indicating a great distribution of nanoparticles and a homogenous state, also confirmed by the macroscopic aspect (see Figure 1).

On the whole, all the values were acceptable in terms of both size and polydispersity and the NAF were proven to be stable within ninety days. Indeed, this agreeable characterization could be again ascribed to the presence of Nafion in the liquid form. Generally, the addition of a liquid lipid in the formulation of nanoparticles allows a better shape of the particle matrix. Hence, the liquid form of lipid in NLC affords the homogeneous and uniform aspect of the final preparation [16].

Recently, nanoparticulate self-assemblies of lipid surfactants in aqueous media received much attention as safe drug delivery systems [17]. Lipid nanocarriers can improve safety of product by solubilizing and stabilizing drug molecules, targeting them to the site of action and/or changing the pharmacokinetics of drugs since lipid based nanomedicines, after systemic administration, distribute differently in the body, and interact differently with biological components at cellular/subcellular level compared to formulations of free drug molecules [17]. Concerning nanoparticles containing ionic interactions it has to be underlined that the toxicity of the system is a good starting point in the evaluation of toxicity and safety. Notably, lipids are physiological compounds characterized by high safety profile, most of them being components of food sources naturally present metabolic pathways for their degradation. Nafion may be a more notable issue in terms of toxicity evaluation since it is a synthetic product and do not find application in pharmaceutical products. In order to evaluate the *in vitro* cytotoxicity, NAF were tested on K562 and A2780 cell lines. Figure 3 graphically shows the percentages of cell growth inhibition generated by NAF on K562 and A2780 cell lines.

On K562 cells was evidenced by a dose-dependent profile up to a concentration of 25  $\mu\text{M}$  getting around 8%.

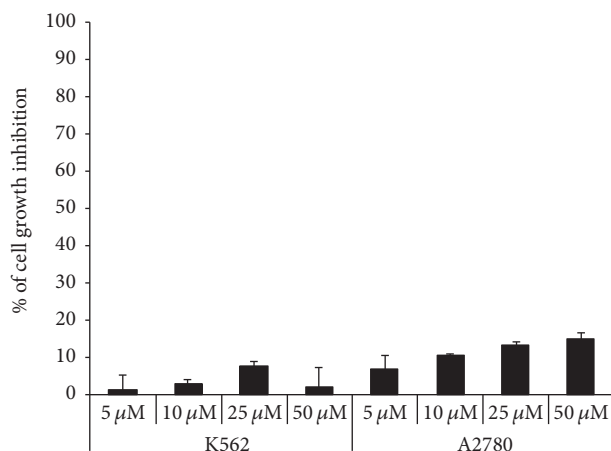


FIGURE 3: *In vitro* antiproliferative effect of NAF on K562 cells and A2780 cells. Data represent the percentages of cell growth inhibition compared to untreated control cells. Data are the mean of three independent experiments  $\pm$  s.d. conducted in triplicate. *P* values are always  $<0.01$ .

On A2780 cells a dose-dependent profile was clearly underlined. The higher percentage of cell growth inhibition was of around 15% using a concentration of 50  $\mu\text{M}$ .

Considering the low values of cell growth inhibition, NAF showed no cytotoxic effect on both cell lines and these results suggest the possibility of studying the interaction with Pt-PTA complexes and the antiproliferative activity as a consequence.

The NAF suspension was characterized by a pH value of  $3.31 \pm 0.15$  (similar to that of an equimolar aqueous solution of Nafion =  $3.01 \pm 0.03$ ). It was mixed to a solution containing a PTA amount equimolar to the concentration of  $-\text{SO}_3\text{H}$  groups. The resulting mixture was subjected to a long scanning  $^{31}\text{P}$  NMR acquisition (18 h), required by the low phosphorus concentration. As demonstrated by the data reported in Table 1, it was found that, after the interaction with NAF, the signal of PTA shifts at  $-90.6$  ppm; the same shift was observed in solution, thus demonstrating the protonating efficiency of nanoparticles containing Nafion and the formation of an ionic interaction between NAF and PTA. This result confirmed our hypothesis of the presence of Nafion sulfonic groups on the surface of the nanoparticles and their ability to form a strong interaction with a proton acceptor.

The ability of NAF/ $\text{PTAH}^+$  to coordinate Pt through the phosphorus site of  $\text{PTAH}^+$  was then checked.  $\text{K}_2\text{PtCl}_4$ , a water soluble source of  $\text{Pt}^{2+}$  (half equivalent with respect to PTA, the expected product being NAF-supported *cis*- $[\text{Pt}(\text{PTAH}^+)_2\text{Cl}_2]$ ), was added to the NAF/ $\text{PTAH}^+$  suspension and  $^{31}\text{P}$  NMR was acquired over 60 hours.

The obtained  $^{31}\text{P}$  NMR spectrum showed a signal shift from  $-90.6$  ppm to  $-49.5$  ppm (typical of Pt-coordinated PTA in a *cis*-geometry) which unequivocally proved the complete loading of platinum and the formation of NAF-supported *cis*- $[\text{Pt}(\text{PTAH}^+)_2\text{Cl}_2]$ .

TABLE 3: Z-average diameter and polydispersity of NAF-supported *cis*-[Pt(PTAH<sup>+</sup>)<sub>2</sub>Cl<sub>2</sub>].

Time (days)	Z-average (nm)	PdI
0	267.7 ± 4.34	0.245 ± 0.01
10	265.4 ± 6.06	0.268 ± 0.06
20	269.3 ± 5.87	0.252 ± 0.01
30	266.1 ± 1.76	0.231 ± 0.01

The observation of Pt-satellites and the Pt-P coupling constant was not possible, because the observed signal was weak and broad, due to the low phosphorus concentration and the probable presence of rapid equilibria.

Concerning their morphology NAF-supported *cis*-[Pt(PTAH<sup>+</sup>)<sub>2</sub>Cl<sub>2</sub>] nanoparticles do not differ from NAF being characterized by ellipsoidal particles or dark rods (data not shown). In addition, as reported in Table 3, in terms of size PCS analysis demonstrated that NAF-supported *cis*-[Pt(PTAH<sup>+</sup>)<sub>2</sub>Cl<sub>2</sub>] nanoparticles are quite stable over a period of 1 month.

#### 4. Conclusions

Considering the results obtained in this study, the following conclusions can be drawn. NAF were found stable during time, with a uniform appearance, a size of around 250 nm, and a polydispersity of around 0.2. The morphological aspect of these nanoparticles was characterized by both ovoidal and needle-like structures, constituting a homogeneous population. The acid pH value of NAF suggested the possibility of protonating PTA; this ability was studied demonstrating the formation of the complex NAF/PTAH<sup>+</sup> which then successfully coordinated Pt. The evaluation of the *in vitro* cell growth inhibition on K562 and A2780 cell lines demonstrated the lack of cytotoxicity of NAF and their promising use as vehicles for Pt-PTA complexes.

Further experiments are necessary to increase the final platinum concentration and to test the antiproliferative activity of Pt-containing NAF/PTAH<sup>+</sup> preparation. Nevertheless, this work represents the first example of pharmaceutically aimed use of Nafion and of the use of electrostatic interactions for nanoparticles functionalization. Moreover, further studies could be aimed at investigating the possibility, in NAF/PTAH<sup>+</sup> preparation, of switching the loading and detaching of platinum by pH or ionic strength modulation.

#### Conflicts of Interest

The authors declare that they have no conflicts of interest.

#### Acknowledgments

This work was supported by grants from the Italian Ministry of University and Research (MIUR) (FIRB2010 to Rita Cortesi). Federica Carducci acknowledges support from Italian FIRB "Future in Research" RBFRI2SIPT MIND.

#### References

- [1] M. Gordon and S. Hollander, "Review of platinum anticancer compounds," *Journal of Medicine*, vol. 24, no. 4-5, pp. 209–265, 1993.
- [2] L. Kelland, "The resurgence of platinum-based cancer chemotherapy," *Nature Reviews Cancer*, vol. 7, no. 8, pp. 573–584, 2007.
- [3] P. Bergamini, V. Bertolasi, L. Marvelli et al., "Phosphinic platinum complexes with 8-thiotheophylline derivatives: synthesis, characterization, and antiproliferative activity," *Inorganic Chemistry*, vol. 46, no. 10, pp. 4267–4276, 2007.
- [4] C. Santini, M. Pellei, G. Papini et al., "In vitro antitumour activity of water soluble Cu(I), Ag(I) and Au(I) complexes supported by hydrophilic alkyl phosphine ligands," *Journal of Inorganic Biochemistry*, vol. 105, no. 2, pp. 232–240, 2011.
- [5] F. Sampedro, A. Molins-Pujol, J. Bonal et al., "Sulfide and phosphine ligands in carboplatin analogs," *European Journal of Medicinal Chemistry*, vol. 26, no. 5, pp. 539–543, 1991.
- [6] S. Guo and L. Huang, "Nanoparticles containing insoluble drug for cancer therapy," *Biotechnology Advances*, vol. 32, no. 4, pp. 778–788, 2014.
- [7] D. J. Daigle, A. B. Pepperman Jr., and S. L. Vail, "Synthesis of a monophosphorus analog of hexamethylenetetramine," *Journal of Heterocyclic Chemistry*, vol. 11, no. 3, pp. 407–408, 1974.
- [8] X. Tang, B. Zhang, Z. He, R. Gao, and Z. He, "1,3,5-Triaza-7-phosphaadamantane (PTA): a practical and versatile nucleophilic phosphine organocatalyst," *Advanced Synthesis & Catalysis*, vol. 349, no. 11-12, pp. 2007–2017, 2007.
- [9] R. Cortesi, C. Damiani, L. Ravani et al., "Lipid-based nanoparticles containing cationic derivatives of PTA (1,3,5-triaza-7-phosphaadamantane) as innovative vehicle for Pt complexes: production, characterization and in vitro studies," *International Journal of Pharmaceutics*, vol. 492, no. 1-2, pp. 291–300, 2015.
- [10] P. Bergamini, L. Marvelli, A. Marchi et al., "Platinum and ruthenium complexes of new long-tail derivatives of PTA (1,3,5-triaza-7-phosphaadamantane): synthesis, characterization and antiproliferative activity on human tumoral cell lines," *Inorganica Chimica Acta*, vol. 391, pp. 162–170, 2012.
- [11] M. Sguizzato, R. Cortesi, E. Gallerani et al., "Solid lipid nanoparticles for the delivery of 1,3,5-triaza-7-phosphaadamantane (PTA) platinum (II) carboxylates," *Materials Science and Engineering: C*, vol. 74, pp. 357–364, 2017.
- [12] R. Pecora, "Dynamic light scattering measurement of nanometer particles in liquids," *Journal of Nanoparticle Research*, vol. 2, no. 2, pp. 123–131, 2000.
- [13] V. Luzzati, H. Delacroix, T. Gulik-Krzywicki, P. Mariani, and R. Vargas, "The cubic phases of lipids," *Current Topics in Membrane*, vol. 44, pp. 3–7, 1997.
- [14] K. A. Mauritz and R. B. Moore, "State of understanding of Nafion," *Chemical Reviews*, vol. 104, no. 10, pp. 4535–4585, 2004.
- [15] G. M. Eccleston, "Emulsions and creams," in *Aulton's Pharmaceutics, The Design and Manufacture of Medicines*, M. E. Aulton and K. M. G. Taylor, Eds., pp. 435–464, Churchill Livingstone Elsevier, London, UK, 4th edition, 2013.
- [16] R. H. Müller, M. Radtke, and S. A. Wissing, "Nanostructured lipid matrices for improved microencapsulation of drugs," *International Journal of Pharmaceutics*, vol. 242, no. 1-2, pp. 121–128, 2002.
- [17] H. Svilenov and C. Tzachev, "Solid lipid nanoparticles—a promising drug delivery system," in *Nanomedicine*, A. Seifalian, A. de Mel, and D. M. Kalaskar, Eds., pp. 187–237, One Central Press, Manchester, UK, 2014.

